RESEARCH ARTICLE
doi: 10.2306/scienceasia1513-1874.2025.008

ScienceAsia 51 (1): 2025: ID 2025008: **1–11**

Anti-inflammatory effect of *Rhamnella gilgitica Mansf*. et Melch on complete Freund's adjuvant induced-arthritis mice and lipopolysaccharide (LPS)-treated RAW264.7 cells by mediating the MAPK signaling pathway

Thubten Sambu[a,†], **Tsering Dikye**[a,†], **Tong Wang**[b], **Liying Gao**[b], **Bin Li**[b], **Shan Huang**[b,*]

[a] The department of Tibetan Medicine, University of Tibetan Medicine, Lhasa 850000 China
[b] Department of Pharmacy, Key Laboratory of Pharmaceutical Research for Metabolic Diseases, Qingdao University of Science & Technology, Qingdao 266042 China

*Corresponding author, e-mail: huangshan@qust.edu.cn
† These authors contributed equally to this work.

Received 27 May 2023, Accepted 19 Dec 2024
Available online 15 Feb 2025

ABSTRACT: Inflammation and oxidation are widely regarded as primary contributors to rheumatoid arthritis, with macrophages such as murine RAW264.7 cells playing significant roles in the disease progression by secreting inflammatory cytokines. *Rhamnella gilgitica Mansf*. et Melch (RG), a traditional Chinese plant medicine, has been shown to have anti-inflammatory and anti-rheumatoid effects, although its underlying mechanism remains unclear. In this study, we confirmed the anti-inflammatory and anti-oxidative effects of RG and investigated its protective mechanism. The active components of RG were analyzed using LC-MS/MS. The components found included ursolic acid, daidzin, simvastatin, chlorogenic acid, casticin, kaempferol, naringenin, azelanic acid, and vanillic acid. In addition, the contents of kaempferol and naringenin were examined by HPLC. Results showed that RG significantly improved ankle joint swelling, arthritis index, paw thickness, and ankle joint thickness; with decreasing serum levels of pro-inflammatory cytokines' such as IL-1β, IL-6, TNF-α, and RF. Furthermore, RG also inhibited the protein expression levels of IL-10 and IL-17, as well as the protein phosphorylation of MAPK signaling pathway including JNK, ERK, and P38 in ankle cartilage of mice. *In vivo*, RG decreased the levels of NO, IL-1β, IL-6, TNF-α. and IL-17. Additionally, RG inhibited the protein phosphorylation of JNK, ERK, and P38 in RAW264.7 cells stimulated by LPS. Overall, results suggested that the underlying anti-inflammatory effects of RG could be associated with the inhibition of JNK, ERK, and P38 protein phosphorylation.

KEYWORDS: *Rhamnella gilgitica Mansf*. et Melch, rheumatoid arthritis, RAW264.7 cells, MAPK, mice

INTRODUCTION

Rheumatoid arthritis (RA) is a chronic autoimmune disease characterized by inflammation, synovitis, cartilage erosion, and bone destruction, which affects around 0.1% of the global population [1, 2]. RA progression is caused by a variety of endogenous and exogenous factors, including genetic and environmental factors, dietary habit, obesity, and bacterial infection [3]. The goals of RA treatment are to reduce pain and inflammation and to prevent cartilage injury and joint deformity [4]. Although nonsteroidal anti-inflammatory drugs, disease-modifying anti-rheumatic drugs, and glucocorticoids effectively relieve pain and inhibit the inflammatory reaction, they are temporarily administrated due to their severe hepatorenal toxicity and other side effects [5, 6]. At the same time, traditional drugs have been proved to be beneficial for RA treatment because of their reliably mild curative effect and low toxicity. Notably, the herb extract ECa 233 has shown promising anti-inflammatory effects on osteoarthritis, particularly at the mandibular joint. The finding was demonstrated in recent studies involving animal models similar to those used for rheumatoid arthritis [7]. Traditional herbs contain various active ingredients that can improve RA symptoms by interacting with immune regulation, inflammatory response, angiogenesis, miRNA, and oxidative stress, together with good anti-RA activity [8]. Hence, the study of traditional medicine for arthritis treatment has become a highlight of researches for many scholars.

Rhamnella gilgitica Mansf. et Melch (RG), a traditional Tibetan medicine belonging to the rhamnaceae plant, is recorded in Shel Gong Shel Phreng, mainly distributed in Qinghai-Tibet Plateau at an altitude of 2600–2900 m. In the Tibetan medical theory, RG is traditionally used to treat rheumatism, swelling, and pain [9]. In our previous study, the anti-rheumatoid arthritis effects of RG have been demonstrated in arthritis rats [10]. *In vitro* experimental data showed that the anti-inflammatory effect of RG was related to inhibition of the NF-κB signaling pathway. Su et al [11] found that the anti-RA effect of RG was to promote cell apoptosis by mediating the expression of JAK/STAT signaling pathway in the synovium region of collagen-induced arthritis rats. The MAPK signaling pathway

has been implicated in the development and deterioration of RA, including cell proliferation, apoptosis, differentiation, and inflammatory responses [12, 13]. Previous studies reported that the anti-rheumatoid effect of RG was mainly and closely related to its anti-inflammatory effect. However, are there any other potential anti-inflammatory action mechanisms about RG? If there are, are they related to the MAPK signaling pathway? Therefore, the main focus of this study was to find the answer to these questions.

MATERIALS AND METHODS

Chemicals and reagents

The tissue culture reagents used in this study: Dulbecco's Modified Eagle's Medium (DMEM) and fetal bovine serum (FBS) were acquired from Gibco BRL (Grand Island, NY, USA). Enzyme-Linked Immunosorbent Assay (ELISA) kits for detecting interleukins (IL)-1β, IL-6, IL-10, and IL-17; tumor necrosis factor (TNF)-α; and rheumatoid factor (RF) were obtained from R&D Systems (Minneapolis, MN, USA). The primary antibodies, p38, p-p38, JNK, p-JNK, ERK, p-ERK, and β-actin; and their respective secondary antibodies were purchased from Cell Signaling Technology (Danvers, MA, USA). Complete Freund's adjuvant (CFA) and other chemicals were acquired from Sigma-Aldrich (St. Louis, MO, USA).

Preparation of RG

Rhamnella gilgitica Mansf. et Melch (RG), was collected in Linzhi City, Tibet, in September 2022 and identified by Professor Jule Wang from Tibet University, China. Pulverized heartwood of RG was subjected to extraction using 70% EtOH as a solvent at a solid/liquid ratio of 1:20 and with two repetitions of 2 h extraction under reflux. The obtained mixture was filtered with filter paper. The filtrate was subsequently evaporated under vacuum to obtain the RG powder. The extraction yield was 6.61%. The RG powder was stored at −20 °C and compiled into the Component Bank of Tibetan Medicine (CBTM-E317).

Analysis of RG main components

RG samples were subjected to UHPLC analysis using a Vanquish UHPLC system (Thermo Fisher Scientific, Waltham, MA, USA) equipped with a UPLC HSS T3 column (2.1 mm × 100 mm, 1.8 μm) and coupled to an Orbitrap Exploris 120 mass spectrometer (Orbitrap MS, Thermo Fisher Scientific). The mobile phase consisted of 5 mmol/l ammonium acetate and 5 mmol/l acetic acid in water (A) and acetonitrile (B). The autosampler temperature was maintained at 4 °C, and the injection volume was 2 μl. RG samples were prepared by weighing 0.1 g of powdered herb into a 10 ml volumetric flask, adding 75% methanol to volume, and ultrasonically extracting at 40 °C for 30 min. The extract was cooled, topped up with 75% methanol, mixed, and centrifuged at 12000 rpm for 10 min. The supernatant was used as the sample solution. The Orbitrap Exploris 120 mass spectrometer was used in information-dependent acquisition (IDA) mode to acquire MS/MS spectra controlled by the Xcalibur software (Thermo Fisher Scientific). In this mode, the acquisition software continuously evaluated the full scan MS spectrum. The ESI source conditions were set as follows: sheath gas flow rate, 50 Arb; Aux gas flow rate, 15 Arb; capillary temperature, 320 °C; full MS resolution, 60000; MS/MS resolution, 15000; collision energy, 10/30/60 eV in Normalized Collision Energy (NCE) mode; and spray voltages, 3.8 kV (positive) or −3.4 kV (negative).

High performance liquid chromatography (HPLC) of RG

Chromatography was conducted through gradient elution on an Agilent 1220 Infinity LC System (Agilent Technologies, USA). Chromatographic separations were performed using a Hypersil BDS C18 column (4.6 × 250 mm, 5 μm, Thermo Fisher Scientific) at 25 °C with a flow rate of 1 ml/min. The mobile phase consisted of acetonitrile (A) and 0.1% phosphoric acid (B). The gradient elution program was set as follow: 15% (A) and 85% (B) for 0–40 min, and 25% (A) and 75% (B) for 40–80 min. Chromatograms were obtained with a UV detector at 360 nm.

Experimental animals

Eighty DBA/1 male mice were procured from the Qingdao Institute for Food and Drug Control (approval number: SYXK (Lu) 2022 0342). All animal experimental procedures were approved by the Institutional Animal Care and Use Committee of Qingdao University of Science and Technology (approval number: ACQUST-2020-056) and were in accordance with the ethical standards. Mice were housed in a clean environment under a controlled 12 h light/12 h dark cycle at a temperature of 22 ± 2 °C, with *ad libitum* access to food and water.

Experimental design

After one week of adaptive feeding, mice were randomly divided into two groups. The first group (n = 10) was designated as normal control group (Con); while the remaining seventy mice, rheumatoid arthritis (RA) group. were induced to develop RA through the subcutaneous injection of 50 μl of complete Freund's adjuvant into the foot pad of the right hind paw. Two weeks after the injection, the RA group mice were randomly divided into five groups (n = 10 per group) according to treatment of drugs: rheumatoid arthritis model (no drug) group (RA); methotrexate group as the positive control (MTX, 1.3 mg/kg/day); low dose-RG group (L-RG, 2047.5 mg/kg/day); middle dose-RG group (M-RG, 4095 mg/kg/day); and high dose-RG

group (H-RG, 8190 mg/kg/day). The drugs (MTX, L-RG, M-RG, and H-RG) were administered once daily via oral gavage. After 4 weeks of treatment and a 12 h fast, mice were euthanized using cervial dislocation, and blood samples were collected for analysis. Spleen, thymus, and ankle cartilage were removed and stored for further experiment. Serum samples were used to measure biochemical parameters. During the experiment, arthritis index scores were assessed every 7 days for all groups; and paw and ankle joint thickness of individual mice were measured. Arthritis scores were assigned based on the following criteria: 0, no redness or swelling of the ankle joint; 1, slight swelling of the ankle; 2, moderate swelling of the ankle with noticeable redness; 3, severe swelling of the whole paw; 4, severe swelling and stiffness of the hind limbs.

Biochemical parameters

ELISA kits obtained from BOSTER Biological Technology (Wuhan, China) were used to detect levels of IL-1β, IL-6, TNF-α, and RF in serum and in cells supernatant.

Histopathological evaluations

Ankle cartilage specimens were fixed with 4% paraformaldehyde for more than 24 h and subsequently embedded in paraffin. The specimens were then sectioned to a thickness of 5 µm and subjected to haematoxylin and eosin (H&E) staining to assess any histopathological alterations.

Immunohistochemistry

Paraffin-embedded tissues were sectioned into 5 µm-thick slices and mounted onto silanized slides, followed by deparaffinization and hydration. Endogenous peroxidase activity was blocked with 3% hydrogen peroxide in methanol. The tissue sections were incubated in 5% normal goat serum in Tris-buffered saline for 60 min and then incubated overnight to a 1:100 dilution of polyclonal goat anti-mouse IL-10, IL-17, p-p38, p-JNK, and p-ERK antibodies, which were obtained from Affinity Biosciences (OH, USA).

Cell culture and the viability assay

RAW264.7 macrophage cell line was obtained from the China Center for Type Culture Collection (Wuhan, China) and maintained in DMEM containing 10% FBS. The cells were routinely cultured in a humidified incubator with 5% CO_2 at 37 °C. RAW264.7 cells were seeded at a density of 8×10^3 cells/well in 96-well plates and incubated for 12 h. Subsequently, the cells were treated with various concentrations of RG for 12 h, followed by treatment with lipopolysaccharide (LPS, 1 µg/ml) for 24 h. Cell viability was examined by adding 50 µl of 3-[4,5-dimethylthiazol-2-yl]-2,5-diphenyltetrazolium bromide (MTT, 2.5 mg/ml) to each well. After 4 h, 150 µl of dimethyl sulfoxide (DMSO) was added to each well to dissolve formazan crystals formed by viable cells. The absorbance of the dissolved formazan was measured at 490 nm. RG was dissolved in DMSO (final culture concentration, 0.05%) for each experiment.

Measurements of levels of inflammatory factors in cells

Cells were harvested and combined with Radioimmunoprecipitation Assay (RIPA) lysis buffer (Solarbio, Beijing, China), after which they were suspended and maintained at 0 °C or on ice for a duration of 9 minutes to promote cell lysis. Following this, the obtained mixture was subjected to centrifugation at $15000 \times g$ for a period of 15 min at 4 °C, yielding a supernatant containing cell extracts. The levels of various cytokines, namely IL-1β, IL-6, IL-17 and TNF-α, were quantified using ELISA kits, and Griess method was used to detect the NO production.

Western blot analysis

The RIPA buffer (Thermo Fisher Scientific) was used to lyse the cells, and the total protein concentration was determined using the BCA protein assay kit. The protein samples were separated by 10%–15% sodium dodecyl sulfate-polyacrylamide gel electrophoresis and transferred onto PVDF membranes (Millipore, Bedford, MA, USA). The membranes were incubated with 5% dried milk for 2 h and subsequently with diluted primary antibody (1:1000) overnight at 4 °C. Following this, the blottings were incubated with an appropriate horseradish peroxidase-coupled goat anti-rabbit or rabbit anti-mouse secondary antibody at room temperature for 1.5 h. Finally, the blottings were visualized using ECL Western Blotting Substrate (Amersham Bioscience, Buckinghamshire, UK) and a ChemiDoc image analyser (4600; Tanon, Shanghai, China).

Statistical analysis

All data were shown as mean ± SD. Differences between two groups were analyzed using a two-tailed t-test. Statistical significance was considered at $p < 0.05$ or $p < 0.01$.

RESULTS

LC-MS analysis of main components of RG

Previous reports have demonstrated that RG are rich in phenolic acids and flavonoid glycosides. In this study, the active constituents of RG were identified through LC/MS analysis, revealing the presence of kaempferol, naringenin, daidzin, ursolic acid, vanillic acid, casticin, azelaic acid, simvastatin, and chlorogenic acid, as summarized in Fig. 1.

HPLC analysis of RG

In our previous study [10], two active components in RG were identified, kaempferol and naringenin.

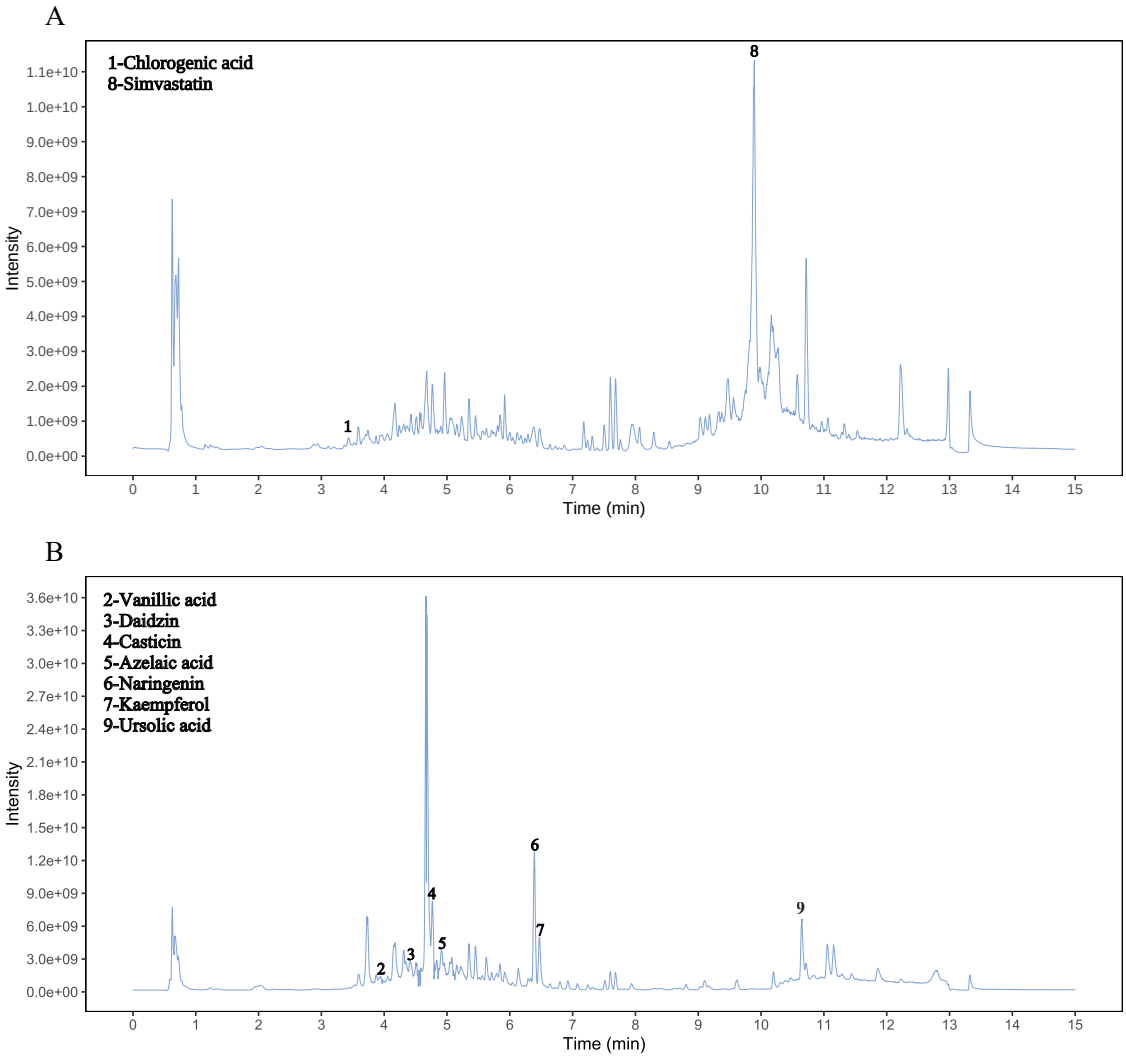

Fig. 1 LC-MS analysis showing main components of RG: A, total positive ion pattern; and B, total negative ion pattern.

Fig. 2A,B show the retention time of two active ingredients in the standard and the extract sample, respectively. The first marked peak was naringenin, and the second one was kaempferol.

Effect of RG on the paw swelling of RA mice

As presented in Fig. 3A, the degree of swelling in the left hind paw of mice was visually assessed. The RA group exhibited a significant increase in swelling compared with the Con group, while the H-RG group demonstrated a noticeable improvement. Moreover, the arthritis index score was determined weekly throughout the experiment. As the study progressed, a decline in the arthritis index score was observed in the RG group (Fig. 3B). Finally, the paw and joint thicknesses were measured, and the results were shown in Fig. 3C,D, respectively. Compared with the Con group, the paw and joint thicknesses of the RA group significantly increased, while the RG-treated mice exhibited a significant decrease in the thicknesses. In addition, we observed that the complete Freund's adjuvant induced a marked increase in the thymus index and spleen index in RA mice, which was dose-dependently reversed by RG treatment (Fig. 3E,F).

Effects of RG on the serum levels of inflammatory factors and cartilage tissue lesion in RA mice

In Fig. 4, the RA group had significantly elevated levels of IL-1β, IL-6, TNF-α, and RF compared with the Con group ($p < 0.05$ or $p < 0.01$). However, RG treatment resulted in a dose-dependent reduction of the serum levels of inflammatory factors, with significant differences compared with the RA group ($p < 0.05$ or $p < 0.01$). As illustrated in Fig. 4E, compared with

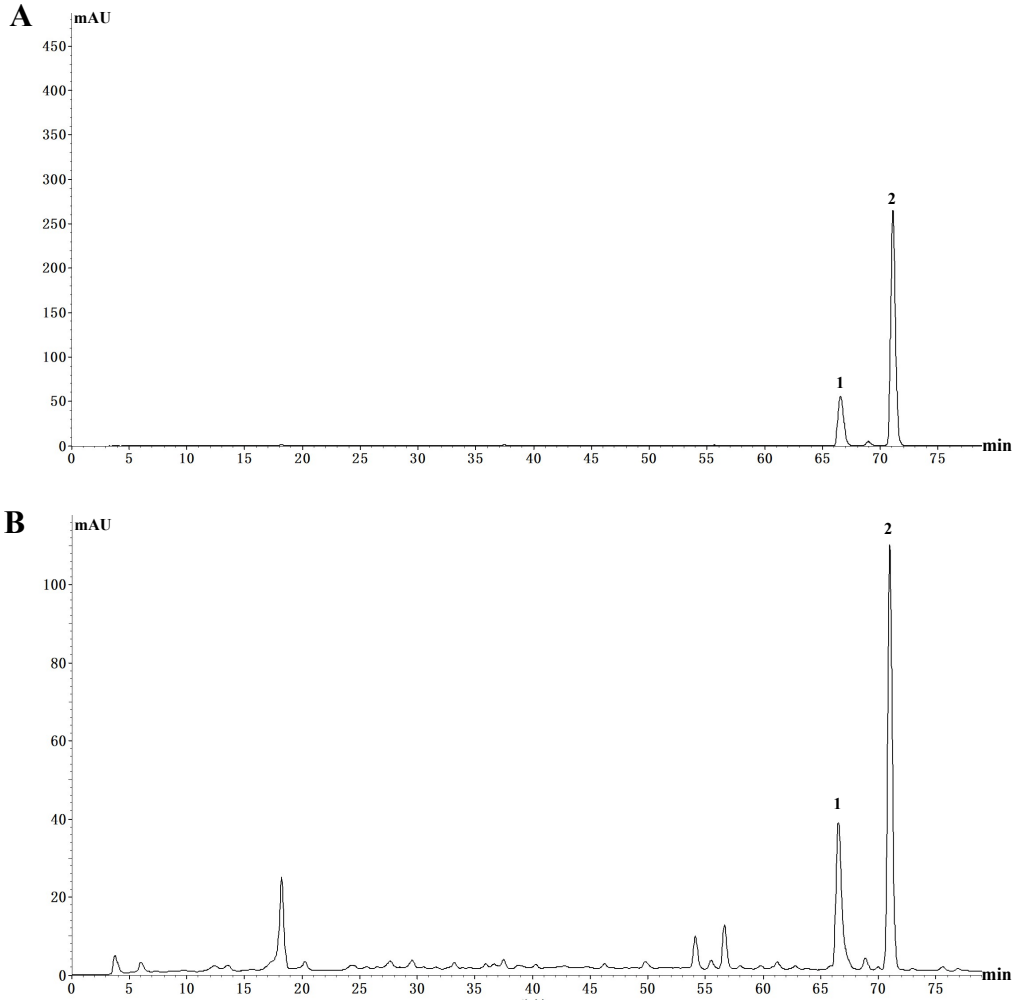

Fig. 2 HPLC analysis of RG: A, chromatogram of the standard; B, chromatogram of the extract; peak 1, naringenin; peak 2, kaempferol.

the Con group, the RA group demonstrated notable inflammatory infiltration in the articular cavity cartilage, with intact articular cartilage tissue. However, the RG group exhibited a substantial improvement in this regard. Saffron O staining revealed the destruction of cartilage tissue structure in the RA group, while cartilage cells in the RG-treated mice were arranged neatly and relatively complete (Fig. 4F).

Effect of RG on protein expressions of inflammatory factors and MAPKs signaling pathway in RA mice

Fig. 5 illustrates that the RA group had a decreased expression level of the IL-10 anti-inflammatory factor and an increased expression level of the IL-17 pro-inflammatory factor, compared with the Con group. Furthermore, the RA group had significantly increased expression levels of phosphorylated P38, JNK, and ERK, whereas treatment with methotrexate or RG significantly increased the expression of IL-10, inhibited the expression of IL-17, and suppressed the phosphorylation of P38, JNK, and ERK.

Effects of RG on the levels of inflammatory factor in LPS-induced RAW264.7 cells

The viability of RAW264.7 cell was evaluated using the MTT assay after treatment with various concentrations of RG (25–400 μg/ml). As depicted in Fig. 6A, treatment with 400 μg/ml of RG resulted in significant cytotoxicity against RAW264.7 cells. Therefore, further experiments were conducted using RG concentrations ranging from 25–200 μg/ml. Fig. 6B to Fig. 6E display the effects of RG on inflammatory factor expressions in LPS-stimulated RAW264.7 cells. LPS stimulation significantly elevated the levels of NO, TNF-α, IL-1β, IL-6, and IL-17 ($p < 0.01$), whereas RG treatment

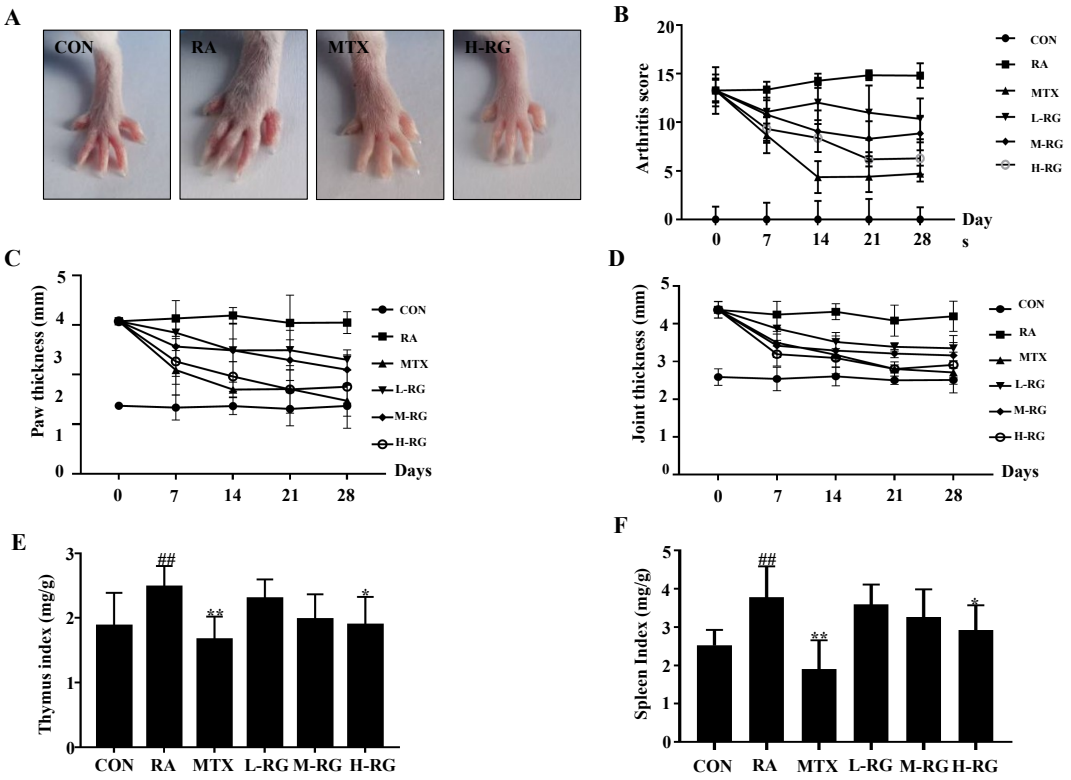

Fig. 3 Effects of RG on the RA mice: A, photos of swelling paws; B, arthritis score; C, paw thickness; D, joint thickness; E, thymus index; and F, spleen index. The mice were treated with different doses of RG for 28 days after CFA inducement. (A) to (D) were measured every 7 days while E and F were assessed post-treatment. Data are mean ± SD, $n = 10$. $^{\#\#}$ $p < 0.01$ vs. CON group, * $p < 0.05$ or ** $p < 0.01$ vs. RA group.

effectively reversed this elevation in a dose-dependent manner ($p < 0.05$ or $p < 0.01$).

Effect of RG on the protein expressions of JNK, ERK, and P38 phosphorylations in RAW264.7 cells

Fig. 7 shows that LPS stimulation significantly increased the phosphorylations of JNK, ERK, and P38 in RAW264.7 cells. However, RG treatment dose-dependently inhibited the phosphorylations of JNK, ERK, and P38 compared with cells treated with LPS alone ($p < 0.05$ or $p < 0.01$).

DISCUSSION

In our previous study, we utilized the HPLC method to identify active components such as quercetin, naringenin, and kaempferol in the ethanol extract of RG [9]; and in this study, naringenin and kaempferol were also identified as the main active components in RG by HPLC. Additionally, we employed LC/MS to further analyze and identify other components of RG. Experimental data revealed that besides naringenin and kaempferol, other active components in RG, e.g., daidzin, ursolic acid, vanillic acid, casticin, azelaic acid, simvastatin, and chlorogenic acid were identified by LC/MS. Many researches have demonstrated that kaempferol, naringenin, ursolic acid, casticin, simvastatin, and chlorogenic acid possess anti-arthritis effects [10], whereas daidzin, vanillic acid, and azelaic acid are known to have prominent anti-inflammatory and antioxidant effects [14–16]. Therefore, the pharmacological activities of these components provide a theoretical basis for RG's anti-arthritis effects.

Currently, there are numerous methods to establish RA animal models. Among these, arthritis induced by complete Freund's adjuvant in mice is one of the classic and commonly used methods. This method is characterized by secondary autoimmune swelling in mice, which is highly similar to that in human patients. The pathogenic mechanism is that the heat shock protein in *Mycobacterium tuberculosis* is highly similar to the proteoglycan bridge protein in articular cartilage, and T cells are activated and mistakenly attack articular cartilage, causing arthrosis lesions [17, 18]. The most intuitive index to judge the drug effect is whether the ankle joint is swollen. In the present study, after complete Freund's adjuvant induction in mice, the swollen joints and the increased thicknesses of paw and ankle joints in the RA mice were observed, indi-

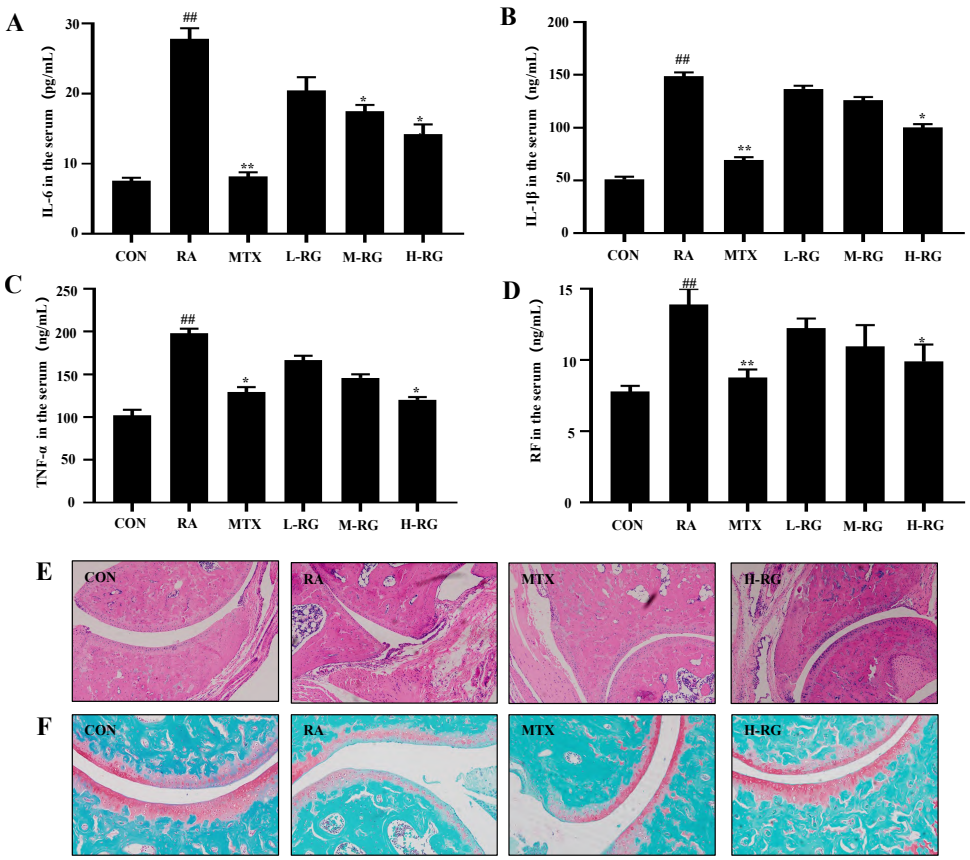

Fig. 4 Effects of RG on the serum levels of pro-inflammatory cytokines and cartilage tissue lesions in RA mice. Serum levels, measured by ELISA, of: A, IL-6; B IL-1β; C, TNF-α; and D, RF. Cartilage tissue lesions: E, analyzed by HE; and F, safranine O-fast green staining. Data are mean ± SD, $n = 10$. $^{\#\#}$ $p < 0.01$ vs. CON group, * $p < 0.05$ or ** $p < 0.01$ vs. RA group.

Table 1 LC-MS analysis of main components of RG.

Number	Tentative Identification	Molecular formula	Rt (min)	Theoretical Mass m/z	MW	m/z Traces(−)	m/z Traces(+)
1	Chlorogenic acid	$C_{16}H_{18}O_9$	3.42	355.1024	354.309		355.0992
2	Vanillic acid	$C_8H_8O_4$	3.90	167.0339	168.147	167.0349	
3	Daidzin	$C_{21}H_{20}O_9$	4.51	415.1024	416.378	415.1028	
4	Casticin	$C_{19}H_{18}O_8$	4.83	373.0918	374.341	373.0932	
5	Azelaic acid	$C_{15}H_{12}O_5$	4.96	187.0965	188.221	187.0976	
6	Naringenin	$C_{15}H_{12}O_5$	6.39	271.0601	272.253	271.0605	
7	Kaempferol	$C_{15}H_{10}O_6$	6.47	285.0394	286.236	285.0402	
8	Simvastatin	$C_{25}H_{38}O_5$	9.89	419.2792	418.566		419.2769
9	Ursolic acid	$C_{30}H_{48}O_3$	10.64	455.3520	456.700	455.3531	

cating that the RA model was successfully established. This conclusion was also confirmed by H&E staining and saffron O staining. Inflammatory cells infiltrated into cartilage tissue of RA mice, and cartilage matrix obviously decreased; while RG treatment effectively restored the aforementioned lesions. As thymus and spleen are important parts of lymphocyte proliferation, differentiation, and maturation; they play important roles in normal immune function. Hence, the thymus index and spleen index can measure the strength of immune function. Complete Freund's adjuvant induction increased the thymus index and spleen index of RA mice, while the intervention of RG decreased both indexes, indicating that RG effectively restored the immune function of the mice.

In the pathogenesis of RA, MI-type pro-

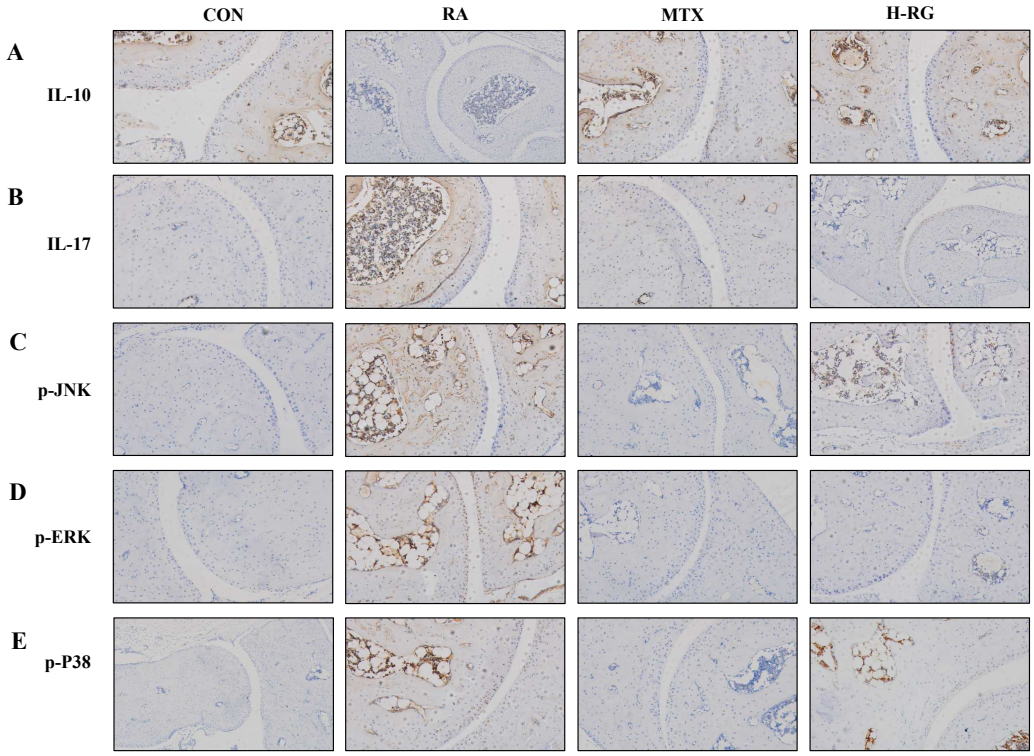

Fig. 5 Effects of RG on protein expressions of inflammatory factors and MAPKs signaling pathway in RA mice treated with different doses of RG for 28 days after CFA inducement. Ankle cartilage protein levels of: A, IL-10; B, IL-17; C, p-JNK; D, p-ERK; and E, p-P38, determined by immunohistochemistry (200× magnification).

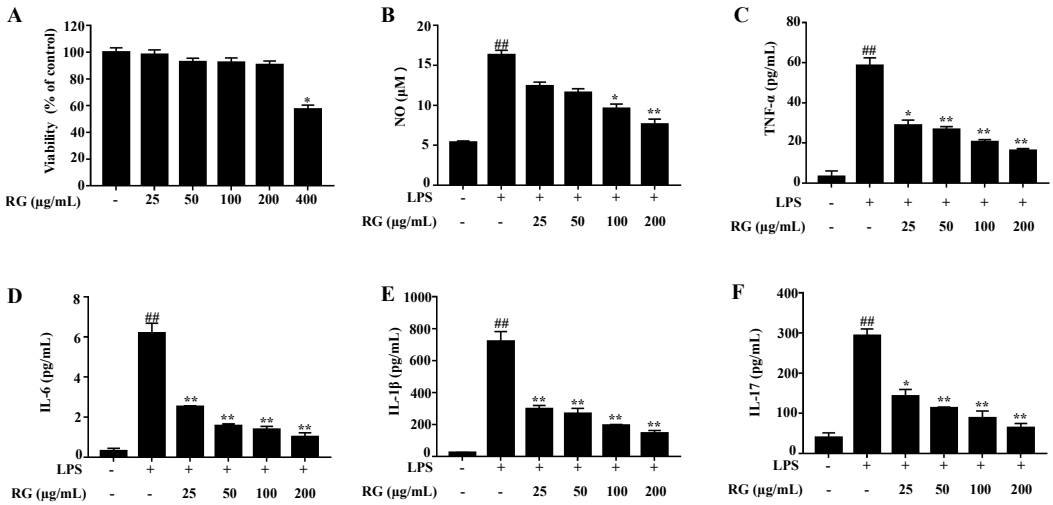

Fig. 6 Effects of RG on the levels of pro-inflammatory factors in LPS-induced RAW264.7 cells. A, Viability of cells treated with various concentrations of RG compared with untreated control (set at 100%); B, nO production; C, TNF-α level; D, IL-6 level; E, IL-1βlevel; and F, IL-17 level. Data are mean ± SD. $^{\#\#}$ $p < 0.01$ vs. control group, * $p < 0.05$ or ** $p < 0.01$ vs. LPS group.

inflammatory macrophages dominate and recruit inflammatory cells, stimulate synovial cell migration and adhesion, induce osteoclast activation, and promote inflammatory response and bone destruction [19, 20]. LPS-induced macrophages are commonly used to establish *in vitro* inflammation models.

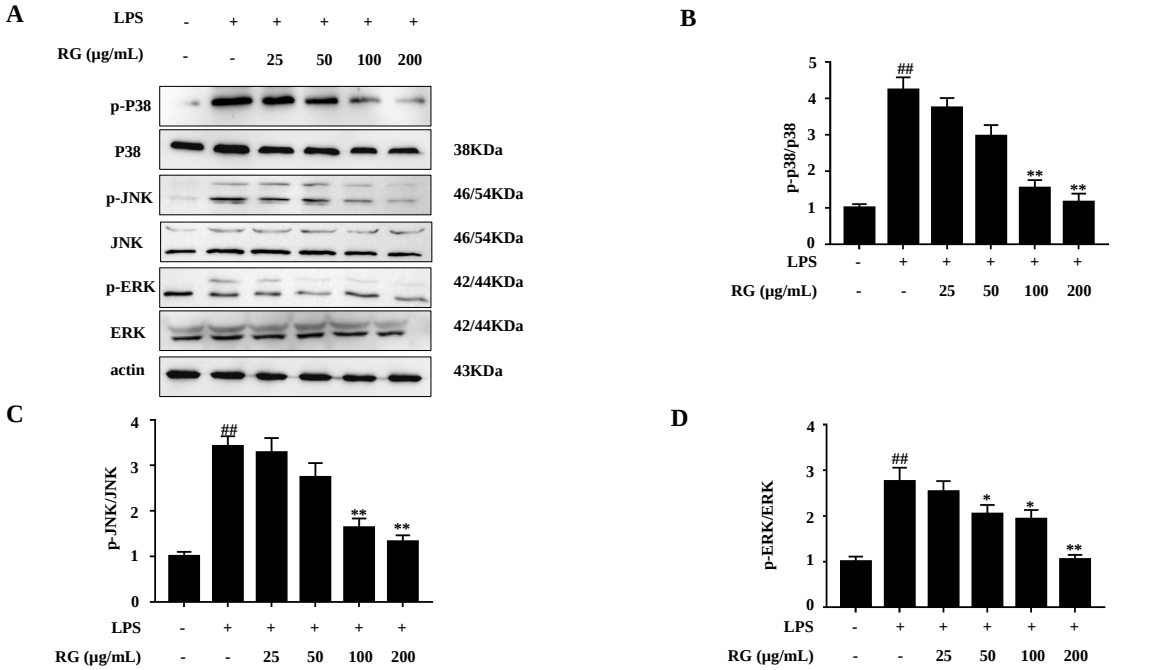

Fig. 7 Effects of RG on the MAPKs signaling pathway in LPS-induced RAW264.7 cells. A, Protein expressions of p-P38, p-JNK, and p-ERK; B, gray value of p-P38; C, gray value of p-JNK; and D, gray value of p-ERK. Data are mean ± SD of three independent experiments. $^{\#\#}$ $p < 0.01$ vs. control group, * $p < 0.05$ or ** $p < 0.01$ vs. LPS group.

Inflammation is the main cause of joint swelling and deterioration, and persistent inflammatory reactions lead to the infiltration of macrophages and recruitment of various inflammatory cells, further enhancing the production of inflammatory factors like ILs and TNF-α, which play a crucial role in initiating synovial hyperplasia and cartilage injury [21, 22]. RF is positively correlated with the development of RA and is clinically used for diagnosis [23]. Our experimental results showed that RG treatment reduced the secretion of TNF-α, IL-1β, IL-6, and RF. Thus, we proposed that RG can improve cartilage injury in RA mice by improving inflammatory response.

In patients with RA, the activation of M1 macrophage occurs in an inflammatory environment dominated by Toll-like receptor (TLR) and interferon (IFN) signaling, which promotes the production of pro-inflammatory cytokines, chemokines, and matrix metalloproteinases, leading to the generation, erosion and progressive joint destruction of osteoclasts [24]. Distinct synovial tissue macrophage subsets can regulate inflammation and remission in RA [25], and Liu et al [26] found that Sinomenine inhibited the progression of rheumatoid arthritis by regulating the form of macrophage subsets. Thus, studying the expression of macrophages and inflammatory factors is of great significance for the treatment of RA. In a previous study on RG, Su et al [11] reported that RG exerted an anti-RA effect by regulating the JAK/STAT signaling pathway to mediate cell inflammation and apoptosis. In our previous study, we demonstrated that RG inhibited LPS-induced macrophages and reduced the secretion of inflammatory factors by suppressing the activation of the NF-κB signaling pathway [10]. However, in this study, we discovered that the MAPK pathway was activated in the cartilage tissue of RA mice and the LPS-stimulated RAW264.7 cells. The MAPK pathway, an essential signaling pathway for the transmission of signals from cell membrane to nucleus, primarily consists of P38, JNK, and ERK. In RA conditions, MAPK activation is closely related to synovial hyperplasia, cartilage injury, and inflammatory reaction; and its phosphorylation usually implies a high level of inflammatory response [27]. Furthermore, it has been proved in many studies that there is a certain correlation among RA, macrophages and MAPK signaling pathway. A study of Lu reported that fargesin blocked M1 macrophage polarization by inhibiting the MAPK pathways and downregulated expression of p-p38 and p-ERK in M1 macrophage [28]. Zhou et al [29] found that Kinsenoside attenuated osteoarthritis by repolarizing macrophages through inactivating MAPK signaling and protecting chondrocytes. Wang et al [30] found that KP-10/Gpr54 attenuated RA through inactivating MAPK signaling in macrophages. Therefore, the activation of the MAPK signaling pathway might

play a positive feedback regulation role in inflammation and oxidative stress in macrophages. Our results showed that after 4 weeks of RG treatment, the phosphorylation expression of MAPK in cartilage tissue of RA mice and in RAW264.7 cells induced by LPS significantly decreased, and the levels of inflammatory factors had been significantly decreased. Therefore, we concluded that RG blocked high-level phosphorylation of the MAPK signaling pathway in macrophages; thereby, weakening the pro-inflammatory effect of macrophages during RA progression and ultimately improving RA. Therefore, the inhibition of MAPK phosphorylation by RG is another potential mechanism to effectively improve RA.

CONCLUSION

In this study, the potential pharmacological mechanism of RG in RA was investigated. The anti-inflammatory and antioxidant effects of RG were evaluated both *in vivo* and *in vitro* experiments. Complete Freund's adjuvant induction-RA mice were used to demonstrate the ameliorative effects of RG on the inflammatory response. *In vitro*, RG was found to significantly inhibit pro-inflammatory factors in RAW264.7 cells induced by LPS. RG has therapeutic effects on RA mainly through anti-inflammatory effects, and these effects are closely related to the inhibition of MAPK signaling pathway. The research results provided a new perspective for further researches and extended applications of RG in the treatment of RA.

Acknowledgements: The work was supported by the National Natural Science Foundation of China (No. 81960775 and No. 82074578).

REFERENCES

1. Mcinnes IB, Schett G (2011) The pathogenesis of rheumatoid arthritis. *N Engl J Med* **365**, 2205–2219.
2. Radu AF, Bungau SG (2021) Management of rheumatoid arthritis: An overview. *Cells* **10**, 2857–2864.
3. Woude DD, Annette HM (2018) Update on the epidemiology, risk factors, and disease outcomes of rheumatoid arthritis. *Best Pract Res Clin Rheumatol* **32**, 174–187.
4. Lin YJ, Anzaghe M, Schülke S (2020) Update on the pathomechanism, diagnosis, and treatment options for rheumatoid arthritis. *Cells* **9**, 880.
5. Huang J, Fu XK, Chen XX (2021) Promising therapeutic targets for treatment of rheumatoid arthritis. *Front Immunol* **12**, 686155.
6. Littlejohn EA, Monrad SU (2018) Early diagnosis and treatment of rheumatoid arthritis. *Prim Care* **45**, 237–255.
7. Rotpenpian N, Wanasuntronwong A, Tapechum S (2022) Efficacy of a standardized *Centella asiatica* (ECa 233) extract against allodynia in a mouse model of temporomandibular osteoarthritis. *ScienceAsia* **48**, 15–22.
8. Wang Y, Chen SJ, Du KZ (2021) Traditional herbal medicine: Therapeutic potential in rheumatoid arthritis. *J Ethnopharmacol* **279**, 114368.
9. Luo DS (2018) *Jing Zhu Materia Medica*, Sichuan Science and Technology Press, Chengdu, China.
10. Huang S, Liu HF, Quan X (2016) *Rhamnella gilgitica* attenuates inflammatory responses in LPS-induced murine macrophages and complete Freund's adjuvant-induced arthritis rats. *Am J Chin Med* **44**, 1379–1392.
11. Su JS, Li QY, Liu J (2021) Ethyl acetate extract of Tibetan medicine *Rhamnella gilgitica* ameliorated type II collagen-induced arthritis in rats via regulating JAK-STAT signaling pathway. *J Ethnopharmacol* **267**, 113514.
12. Li LC, Pan ZH, Ning DS (2021) Rosmanol and carnosol synergistically alleviate rheumatoid arthritis through inhibiting TLR4/NF-κB/MAPK pathway. *Molecules* **27**, 78.
13. Yang GL, Chang CC, Yang YW (2018) Resveratrol alleviates rheumatoid arthritis via reducing ROS and inflammation, inhibiting MAPK signaling pathways, and suppressing angiogenesis. *J Agric Food Chem* **66**, 12953–12960.
14. Wu KC, Lin WY, Sung YT (2019) *Glycine tomentella-hayata* extract and its ingredient daidzin ameliorate cyclophosphamide-induced hemorrhagic cystitis and oxidative stress through the action of antioxidation, antifibrosis, and anti-inflammation. *Chin J Physiol* **62**, 188–195.
15. Hu RZ, Wu SS, Li BZ (2022) Dietary ferulic acid and vanillic acid on inflammation, gut barrier function and growth performance in lipopolysaccharide-challenged piglets. *Anim Nutr* **8**, 144–152.
16. Xiao F, Cui H, Zhong X (2016) Beneficial effect of daidzin in dry eye rat model through the suppression of inflammation and oxidative stress in the cornea. *Saudi J Biol Sci* **25**, 832–837.
17. Dube JY, Mclntosh F, Zarruk JG (2022) Synthetic mycobacterial molecular patterns partially complete Freund's adjuvant. *Sci Rep* **10**, 5874.
18. Zhang WB, Lyu J, Xu JX (2021) The related mechanism of complete Freund's adjuvant-induced chronic inflammation pain based on metabolomics analysis. *Biomed Chromatogr* **35**, e5020.
19. Kurowska-Stolarska M, Alivernini S (2022) Synovial tissue macrophages in joint homeostasis, rheumatoid arthritis and disease remission. *Nat Rev Rheumatol* **18**, 384–397.
20. Siouti E, Andreakors E (2019) The many facets of macrophages in rheumatoid arthritis. *Biochem Pharmacol* **165**, 152–169.
21. Deroyer C, Poulet C, Paulissen G (2022) CEMIP (KIAA1199) regulates inflammation, hyperplasia and fibrosis in osteoarthritis synovial membrane. *Cell Mol Life Sci* **79**, 260.
22. Binder NB, Puchner A, Niederreiter B (2013) Tumor necrosis factor-inhibiting therapy preferentially targets bone destruction but not synovial inflammation in a tumor necrosis factor-driven model of rheumatoid arthritis. *Arthritis Rheum* **65**, 608–617.
23. Petrovská N, Prajzlerová K, Vencovsk J (2021) The preclinical phase of rheumatoid arthritis: From risk factors to prevention of arthritis. *Autoimmun Rev* **20**, 102797.
24. Cutolo M, Campitiello R, Gotelli E (2022) The role of M1/M2 macrophage polarization in rheumatoid arthritis synovitis. *Front Immunol* **13**, 867260.
25. Alivernini S, MacDonald L, Elmesmari A (2020) Distinct synovial tissue macrophage subsets regulate inflamma-

tion and remission in rheumatoid arthritis. *Nat Med* **26**, 1295–1306.

26. Liu W, Zhang Y, Zhu W (2018) Sinomenine inhibits the progression of rheumatoid arthritis by regulating the secretion of inflammatory cytokines and monocyte/-macrophage subsets. *Front Immunol* **9**, 2228.
27. Behl T, Upadhyay T, Singh S (2021) Polyphenols targeting MAPK mediated oxidative stress and inflammation in rheumatoid arthritis. *Molecules* **26**, 6570.
28. Lu J, Zhang H, Pan J (2021) Fargesin ameliorates osteoarthritis via macrophage reprogramming by down-regulating MAPK and NF-κB pathways. *Arthritis Res Ther* **23**, 142.
29. Zhou F, Mei J, Han X (2019) Kinsenoside attenuates osteoarthritis by repolarizing macrophages through inactivating NF-κB/MAPK signaling and protecting chondrocytes. *Acta Pharm Sin B* **9**, 973–985.
30. Wang D, Wu Z, Zhao C (2021) KP-10/Gpr54 attenuates rheumatic arthritis through inactivating NF-κB and MAPK signaling in macrophages. *Pharmacol Res* **171**, 105496.